doi:10.1016/j.jmb.2004.06.057 J. Mol. Biol. (2004) 341, 1367–1379

JMB

Available online at www.sciencedirect.com

SCIENCE DIRECT®

ELSEVIER

Binding of Polyubiquitin Chains to Ubiquitin-associated (UBA) Domains of HHR23A

Shahri Raasi[1], Irina Orlov[2], Karen G. Fleming[3] and Cecile M. Pickart[1]*

[1]*Department of Biochemistry and Molecular Biology/Bloomberg School of Public Health, Johns Hopkins University, 615 North Wolfe Street, Baltimore, MD 21205 USA*

[2]*Biacore, Inc., Piscataway NJ 08854, USA*

[3]*T.C. Jenkins Department of Biophysics/School of Arts and Sciences, Johns Hopkins University, 615 North Wolfe Street, Baltimore, MD 21205 USA*

**Corresponding author*

Ubiquitin-associated (UBA) domains are small protein domains that occur in the context of larger proteins and are likely to function as inter- and intramolecular communication elements in ubiquitin/polyubiquitin signaling. Although monoubiquitin/UBA complexes are well characterized, much less is known about UBA/polyubiquitin complexes, even though polyubiquitin chains are believed to be biologically relevant ligands of many UBA domain proteins. Here, we report the results of a quantitative study of the interaction of K48-linked polyubiquitin chains with UBA domains of the DNA repair/proteolysis protein HHR23A, using surface plasmon resonance and other approaches. We present evidence that the UBL domain of HHR23A negatively regulates polyubiquitin/UBA interactions and identify leucine 8 of ubiquitin as an important determinant of chain recognition. A striking relationship between binding affinity and chain length suggests that maximum affinity is associated with a conformational feature that is fully formed in chains of $n=4$–6 and can be recognized by a single UBA domain of HHR23A. Our findings provide new insights into polyubiquitin chain recognition and set the stage for future structural investigations of UBA/polyubiquitin complexes.

Keywords: polyubiquitin; SPR; Rad23; UBA

Introduction

Ubiquitin, a small and structurally robust protein, regulates diverse cellular processes through its conjugation to other cellular proteins.[1] An enzymatic cascade consisting of ubiquitin-activating enzyme (E1), a ubiquitin-conjugating enzyme (E2), and a ubiquitin protein ligase (E3) links the carboxyl group of Ub-G76 to lysine residues of cellular proteins, including ubiquitin itself.[2,3] The resulting mono- or polyubiquitin signal causes a change in the stability, localization, or activity of the acceptor protein. The best-studied consequence of polyubiquitination is to target proteins to the 26 S proteasome, which binds substrate-linked polyubiquitin chains assembled through K48–G76 isopeptide bonds and degrades the substrate polypeptide chain.[4,5]

Besides Ub–K48, K29 and K63 are also involved in polyubiquitin signaling. In contrast to K29 and K48-linked chains, which signal proteasome-dependent degradation,[5–7] K63-linked chains have been implicated in non-proteolytic pathways, including DNA damage tolerance,[8–10] IκBα kinase activation,[11] and translational regulation.[12] K29, K48, and K63-linked homopolymers can be assembled *in vitro* and there is evidence for K48 and K63-linked homopolymers *in vivo*.[5,9,13] It is not yet known if heteropolymers exist within cells and contribute to polyubiquitin signaling. A recent study detected all seven possible ubiquitin–ubiquitin linkages in budding yeast, suggesting that further polyubiquitin signals remain to be discovered.[3]

Although much is known about specificity in ubiquitin conjugation, understanding of the molecular principles governing (poly)ubiquitin recognition has lagged behind. The recent discovery of several ubiquitin-interacting domains, including the ubiquitin-associated (UBA) domain,[14] the

Abbreviations used: BSA, bovine serum albumin; BS^3, bis(succinimidyl) suberate; EDC, *N*-ethyl-*N*′-(dimethyl-amino-propyl)-carbodiimide; GST, glutathione-*S*-transferase; HBS, Hepes-buffered saline; NHS, *N*-hydroxysuccinimide; R_L, level (in resonance units (RU)) of ligand immobilized on a sensor chip; R_{max}, maximum response (in RU) expected at saturating analyte concentration; SPR, surface plasmon resonance; Ub, ubiquitin; Ub_n, polyubiquitin chain composed of *n* ubiquitin units.

E-mail address of the corresponding author: cpickart@jhmi.edu

0022-2836/$ - see front matter

ubiquitin-interacting motif[15] (UIM), and the CUE domain[16] (coupling of ubiquitin conjugation to endoplasmic reticulum degradation) offers a new opportunity to investigate molecular mechanisms of ubiquitin recognition. These small domains occur in the context of larger proteins and are likely to function as inter- and/or intramolecular communication elements in ubiquitin signaling.

The UBA domain, a degenerate motif of 40–50 amino acid residues, was discovered in a bioinformatic analysis of ubiquitin pathway enzymes and proposed as a potential ubiquitin-interacting element.[14] Concurrently, this property was demonstrated experimentally for the UBA domain of p62.[17] Additional ubiquitin/UBA interactions have been established through *in vitro* and *in vivo* analyses of several other UBA domain proteins.[18,19] A number of UBA domain proteins are known to bind K48-linked polyubiquitin chains in strong preference to monoubiquitin, as first shown by Wilkinson and co-workers.[20] Many UBA domain-containing proteins also contain a ubiquitin-like (UBL) domain that adopts a ubiquitin fold and can interact with a specific subunit of the 26 S proteasome.[21–23] These UBL-UBA proteins have been suggested to deliver polyubiquitinated proteins to proteasomes[20,24] and the degradation of certain model proteasome substrates is indeed dependent on UBL-UBA proteins.[25–27] In other cases, however, UBL-UBA proteins inhibit proteasomal degradation, presumably by hindering access to substrate-linked polyubiquitin chains.[28–30]

Human Rad23A (called HHR23A) functions in nucleotide excision repair and proteasome-dependent proteolysis of certain substrates.[24,28,31,32] Solution structural studies have shown that HHR23A consists of several independently folded domains, including the two UBA domains, which are separated by unstructured regions.[31] Each UBA domain folds into a compact three-helix bundle with a hydrophobic surface patch.[33–35] The UBA domain of p62 and, surprisingly, two CUE domains are also three-helix bundles with a hydrophobic surface patch.[36–38] Ubiquitin has a hydrophobic patch across the surface of its five-stranded β-sheet, which includes the functionally important side-chains of L8, I44, and V70.[39–41] It has been suggested that ubiquitin/UBA interactions are mediated by contacts involving the hydrophobic surface patches of each protein.[35] Such interfaces are indeed present in CUE/monoubiquitin[37,38] and UBA/monoubiquitin[32,42,43] complexes. However, while this model could explain the preferential binding of UBA domains to poly- *versus* monoubiquitin,[19,20,26,44] it does not explain why certain UBA domains prefer to bind one type of polyubiquitin chain over another.[28]

Here, we report the results of a quantitative study of the interaction of polyubiquitin chains with UBA domains of HHR23A using several approaches, including surface plasmon resonance (SPR) which offers a powerful method to measure molecular binding affinities in real time.[45–47] We present evidence that the UBL domain of HHR23A negatively regulates polyubiquitin/UBA interactions and identify ubiquitin's leucine 8 side-chain as an important determinant of chain recognition by an HHR23A-UBA domain. A pronounced relationship between binding affinity and chain length suggests that maximum affinity is associated with a conformational feature that is fully formed in chains of $n = 4$–6, which can be recognized by a single UBA domain of HHR23A. Our findings provide new insights into the molecular properties of UBA/polyubiquitin interactions.

Results

Linkage-specific binding of Ub_4 to HHR23A-UBA domains

In an earlier study we used *in vitro* pull-down assays to demonstrate preferential binding of HHR23A-UBA domains to Ub_4 linked through K48 (*versus* other lysine residues).[28] We supported this conclusion with preliminary SPR experiments that monitored the binding of one concentration of different Ub_4 chains to the dual-UBA domain protein R23D (Figure 1a) immobilized by amine coupling at a high density.[28] With such a high-density surface, the analyte may re-bind during the dissociation phase, leading to an artificially slow rate and a failure to achieve full dissociation.[45] Such an effect is apparent in Figure 7 of our earlier study.[28]

To quantify the binding of a single UBA version of HHR23A to Ub_4 accurately, we prepared a low-density surface ($R_L \sim 300$ RU) by amine-coupling a mutant version of HHR23A that was truncated after the first UBA domain (UBL-UBA1; Figure 1a). As shown in Figure 1b for representative concentrations of K48- and K63-Ub_4, this surface afforded reproducible binding with fast on and off rates. Experiments with a series of Ub_4 concentrations yielded $K_d = 9$ μM for K48-Ub_4, as determined by fitting to a simple 1 : 1 binding model (Figure 1c). K63-Ub_4 bound to UBL-UBA1 with a fourfold reduced affinity ($K_d = 40$ μM; Figure 1c). A different experiment with independently synthesized K48-Ub_4 gave a somewhat higher affinity ($K_d = 3.2$ μM; Figure 2b). The difference may reflect a variation in the properties of the distal ubiquitin moieties of the K48-linked chains used in the two experiments (see Materials and Methods), since the reproducibility of K_d values between experiments was otherwise excellent (see Table 1 and Figure 5). We conclude that HHR23A-UBL-UBA1 binds K48-linked Ub_4 four- to tenfold more tightly than the K63-linked polymer, explaining the difference in binding observed in earlier pull-down assays.[28] Importantly, the earlier studies showed that this specificity applies to a glutathione-*S*-transferase (GST)-fused version of UBA2 and to versions of HHR23A that contain two UBA domains.

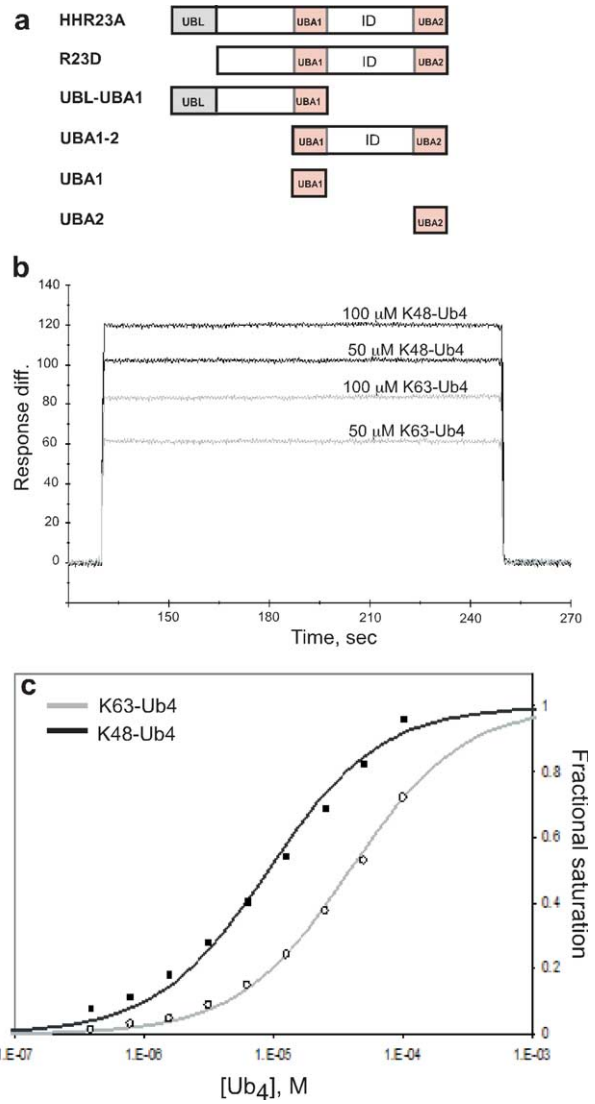

Figure 1. Linkage specificity of polyubiquitin chain binding to HHR23A-UBA1 (SPR). a, Schematic representation of full-length HHR23A protein and the deletion mutants used here. b, Subtracted sensorgrams of the interaction of 50 μM and 100 μM K48-Ub_4 (black traces) compared to K63-Ub_4 (gray traces) as analytes on amine-coupled UBL-UBA1 surface. c, K_d determination: filled squares, K48-Ub_4; open circles, K63-Ub_4. The lines were calculated assuming 1 : 1 binding with $K_d = 9$ μM (black) or 40 μM (gray).

The affinity of K48-Ub_4 for HHR23A-UBL-UBA1 ($K_d = 3.2$–9 μM) is considerably weaker than the affinity of the same chain for Mud1, a fission yeast protein containing a single UBA domain ($K_d = 30$ nM).[20] Thus, different UBA domains apparently vary in their polyubiquitin chain interaction properties. However, inspection of the Mud1 data also suggests that analyte re-binding may have occurred in this experiment, since the observed responses did not return to baseline during the dissociation phase.[20] This effect could have led to some overestimation of the affinity of Mud1 for Ub_4.

Table 1. Length dependence of K48-linked polyubiquitin chain binding to HHR23A-UBA domains

		K_d, (μM)	
n	Analyte mass (kDa)	UBL-UBA1	UBA1-2
2	17	30.2 ± 0.9	ND
3	25.5	9.46 ± 1.0	ND
4	34	3.24 ± 0.3	1.5 ± 0.09[a]
6	51	0.88 ± 0.2	0.089 ± 0.007
8	68	0.52 ± 0.01	0.029 ± 0.005
12	102	0.30 ± 0.03	ND

All values were determined by SPR with the chain as analyte. K_d values were calculated assuming a 1 : 1 stoichiometry (see Materials and Methods). The UBL-UBA1 ligand was amine-coupled; Ub_2, Ub_3, Ub_4, and Ub_6 were analyzed on a surface of $R_L = 370$ RU, while Ub_8 and Ub_{12} were analyzed on a surface of $R_L = 200$ RU. For UBA1-2, the GST-fused ligand was captured by affinity on an anti-GST chip. ND, not determined.
[a] $K_d = 1.3$ μM for the Ub_4/R23D complex (Figure 5a).

Chain binding to UBL-UBA1: affinity, chain length dependence, and stoichiometry

The affinity of K48-linked chains for 26 S proteasomes is length-dependent, with a chain of four ubiquitin molecules constituting the minimum signal for high-affinity binding and efficient degradation.[48] In contrast to the well-studied behavior of different-length chains in proteasome binding, the significance of chain length for UBA domain interactions has not been previously explored. Knowledge of this dependence could provide an important constraint in developing molecular models for binding and biological function.

To address this question, we prepared K48-linked polyubiquitin chains (Ub_n) of $n = 2$, 3, 4, 6, 8, and 12 and utilized UBL-UBA1 as the ligand in order to compare the binding of different chains to a protein containing a single UBA domain. Figure 2a shows raw binding data for Ub_8, confirming rapid binding and complete dissociation. The results summarized in Figure 2b and c and Table 1 reveal a dramatic increase in affinity with increasing chain length. The relationship between affinity and chain length is biphasic: the K_d value falls by ~100-fold as n increases from 1 to 6, but decreases only by threefold more as n increases from 6 to 12 (Table 1 and Figure 2c). Although we did not determine the K_d value for monoubiquitin, extrapolation of the data shown in Figure 2c to $n = 1$ suggests $K_d \sim 100$ μM for monoubiquitin (broken line). This may be compared to $K_d = 400$–500 μM estimated by NMR for the isolated HHR23A-UBA1 and UBA2 domains.[43,49]

To confirm the affinity and probe the stoichiometry of the UBL-UBA1/Ub_4 complex, we evaluated the formation of the complex using sedimentation equilibrium analytical ultracentrifugation. Sedimentation equilibrium is a thermodynamically rigorous method for directly determining molecular mass(es), stoichiometries, and stabilities of complexes in solution. When evaluated individually,

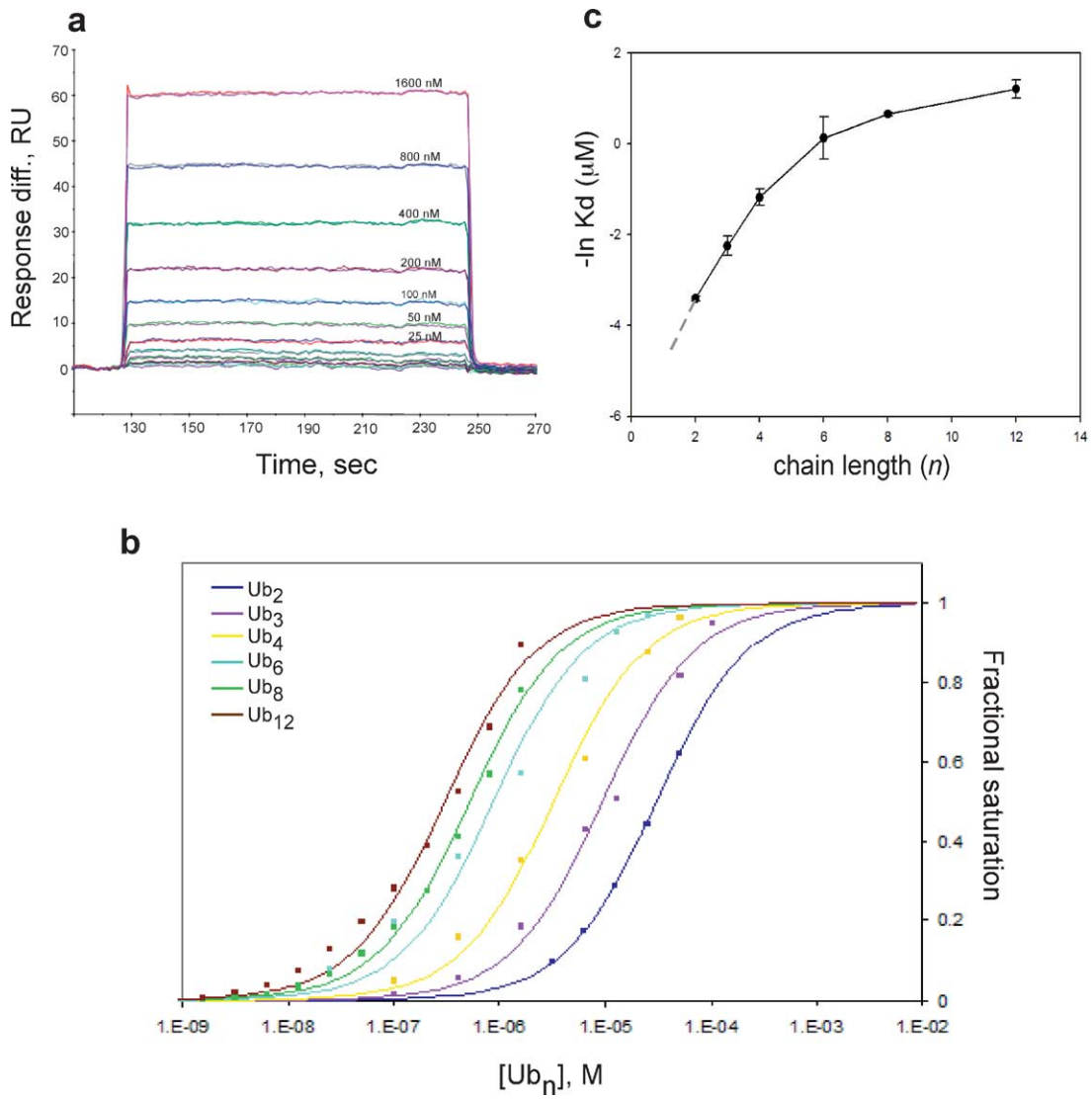

Figure 2. Length dependence of K48-linked polyubiquitin chain binding to the HHR23A-UBL-UBA1 (SPR). a, Subtracted sensorgrams for binding of the indicated concentrations of Ub_8 (each in duplicate) binding to the amine-coupled UBL-UBA1 surface. b, K_d determinations. Sensorgrams for Ub_2, Ub_3, Ub_4, Ub_6, Ub_8, and Ub_{12} were acquired (as in a) and the data analyzed as for Figure 1c. See Table 1 for K_d values. c, Dependence of ($-\ln K_d$) on chain length (n).

both UBL-UBA1 and Ub_4 were found to be completely monomeric at micromolar concentrations. The nature of the complex between them was evaluated by sedimentation equilibrium analysis of a 1 : 2 molar ratio mixture of UBL-UBA1/Ub_4. As shown in Figure 3, an excellent fit to the data was obtained using the equations describing a 1 : 1 stoichiometry with $K_d = 3$ μM. The value of K_d is identical with the value obtained for the same chain by SPR (Table 1), while the stoichiometry is in agreement with the results of cross-linking experiments (see below) and with the model used to fit the SPR data. To further verify this stoichiometry, we tried to fit the data using the equations describing a complex with a 2 : 1 or a 4 : 1 UBL-UBA1/Ub_4 stoichiometry; however, these models did not describe the data well and were rejected (data not shown).

We used chemical cross-linking as a further probe of the stiochiometry of UBL-UBA1 complexes with K48-linked chains. UBL-UBA1, with a true molecular mass of 22.1 kDa, migrates with an anomalous mass of ~35 kDa during SDS-PAGE[28] (Figure 4a, lane 1). In cross-linking experiments performed with Ub_2, the sole cross-linked product observed by Coomassie staining (lane 2) or Western blotting (not shown) migrated with an apparent mass of ~48 kDa, close to the mass of ~52 kDa expected for a 1 : 1 complex. This experiment was done under sub-saturating conditions due to the relatively low affinity of UBL-UBA1 for Ub_2. However, cross-linking of excess UBL-UBA1 to Ub_4 under saturating conditions for this complex also detected a 1 : 1 complex as the principal product, as inferred from Coomassie staining (~68 kDa; Figure 4b, lane 3) or Western blotting with anti-HHR23A antibody (Figure 4c, lanes 2–4). Similar results were obtained at saturation for the UBL-UBA1/Ub_6 interaction

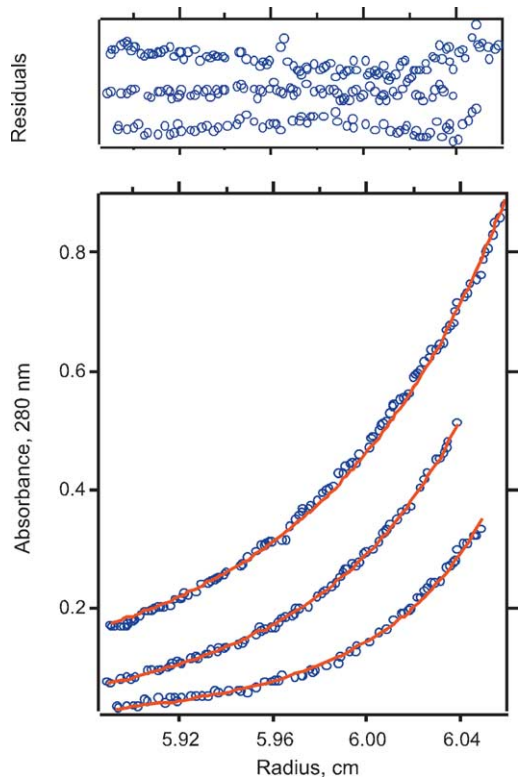

Figure 3. Analytical ultracentrifugation analysis of the UBL-UBA1/Ub_4 interaction. Representative sedimentation equilibrium data for UBL-UBA1/Ub_4. The lower panel shows the data (open circles) and the results of the global fit at 20,000, 24,500 and 30,000 rpm (continuous line) of 1 : 1 association model with $K_d = 3$ μM. The upper panels show the residuals of the fit for these data sets. These represent the difference between the fit and the data and should be small and random, which they are. For clarity these have been offset from each other; however, they are all centered about zero.

(Figure 4c, lanes 7–9). Small amounts of putative 2 : 1 complexes (Figure 4c, triple asterisks) were detected by this more sensitive method, but they were minor products even at high [UBL-UBA1]/[chain] ratios (Figure 4c). Cross-linking experiments conducted at saturation for the UBA2/Ub_4 complex similarly yielded a 1 : 1 complex as the principal product, although a low yield of a 2 : 1 product could be detected at [UBA2]/[Ub_4] = 4 (Figure 4d).

The cross-linking data are in agreement with the 1 : 1 stoichiometry of the UBL-UBA1/Ub_4 complex observed in analytical ultracentrifugation (Figure 3). The data suggest that a chain of $n \leq 6$ complexes optimally with one molecule of UBL-UBA1 or UBA2. The data presented in Figures 2–4 argue against a model in which the principal mode of binding involves each ubiquitin in the chain interacting with one UBA domain.

Polyubiquitin chain binding to dual-UBA versions of HHR23A

Our previous finding that both UBA domains must be present for potent proteasome inhibition by HHR23A[28] led us to examine polyubiquitin chain binding to versions of HHR23A that carried two UBA domains. Our initial studies involved the UBL-deleted protein called R23D (Figure 1a). Using an amine-coupled R23D surface we observed twofold tighter binding of Ub_4 relative to the binding seen on an amine-coupled UBL-UBA1 surface (Figure 5a and Table 1). Experiments with Ub_3 as analyte showed a similar threefold difference between the amine-coupled UBL-UBA1 and R23D surfaces (data not shown). The modest difference in K_d values for UBL-UBA1 *versus* dual-UBA proteins and the absence of cooperative behavior suggests that a second UBA domain enhances Ub_3 and Ub_4 binding mainly through a concentration effect.

This interpretation assumes that the two UBA domains of HHR23A bind similarly to polyubiquitin chains. To test this model, we immobilized Ub_6 by amine coupling and compared the minimal UBA1 and UBA2 domains as analytes. The two UBA domains are similar to or identical with the constructs used in published NMR studies.[43,49] We found that UBA1 and UBA2 indeed behaved similarly, but each displayed a relatively low affinity for Ub_6. The observed K_d values (Supplementary Material, Figure 1) were 30 to 40-fold weaker than the K_d value of the UBL-UBA1/Ub_6 complex as measured in the reverse coupling mode (Table 1).

Since numerous earlier studies have shown that the UBA domains are responsible for chain binding by HHR23A,[18,44,50] this weak binding was unexpected. One possibility is that intramolecular interactions with other regions of HHR23A enhance chain binding to the UBA domains. However, intramolecular UBA interactions were not detected, except inhibitory interactions with the UBL domain (discussed below), in NMR studies of HHR23A.[31] Another possibility is that the minimal UBA domains experience a subtle loss of folding integrity, for example through fraying of the ends of the α1 and α3 helices such as observed to occur by NMR.[31,33,35] This might lead to a non-specific decrease in affinity relative to the same UBA domains in the context of longer proteins such as UBL-UBA1, HHR23A, or even GST-UBA. We favor the second explanation because GST-fused versions of UBA2 and UBL-UBA1 pull down similar amounts of K48-Ub_4 under conditions in which the pull-down signal is sensitive to K_d.[28] While further work is needed to determine if specific or non-specific effects account for the stronger affinity of UBL-UBA1 compared to UBA1, the results obtained with UBA1 and UBA2 offer a preliminary indication that the two UBAs do not differ markedly in their affinities for polyubiquitin chains. This inference is consistent with the results of previous pull-down experiments.[28]

In investigating the binding of longer chains to dual-UBA proteins, we were concerned about a possible requirement for flexibility of the ligand surface. Therefore, we also conducted experiments with GST-fused UBA1-2 immobilized by affinity

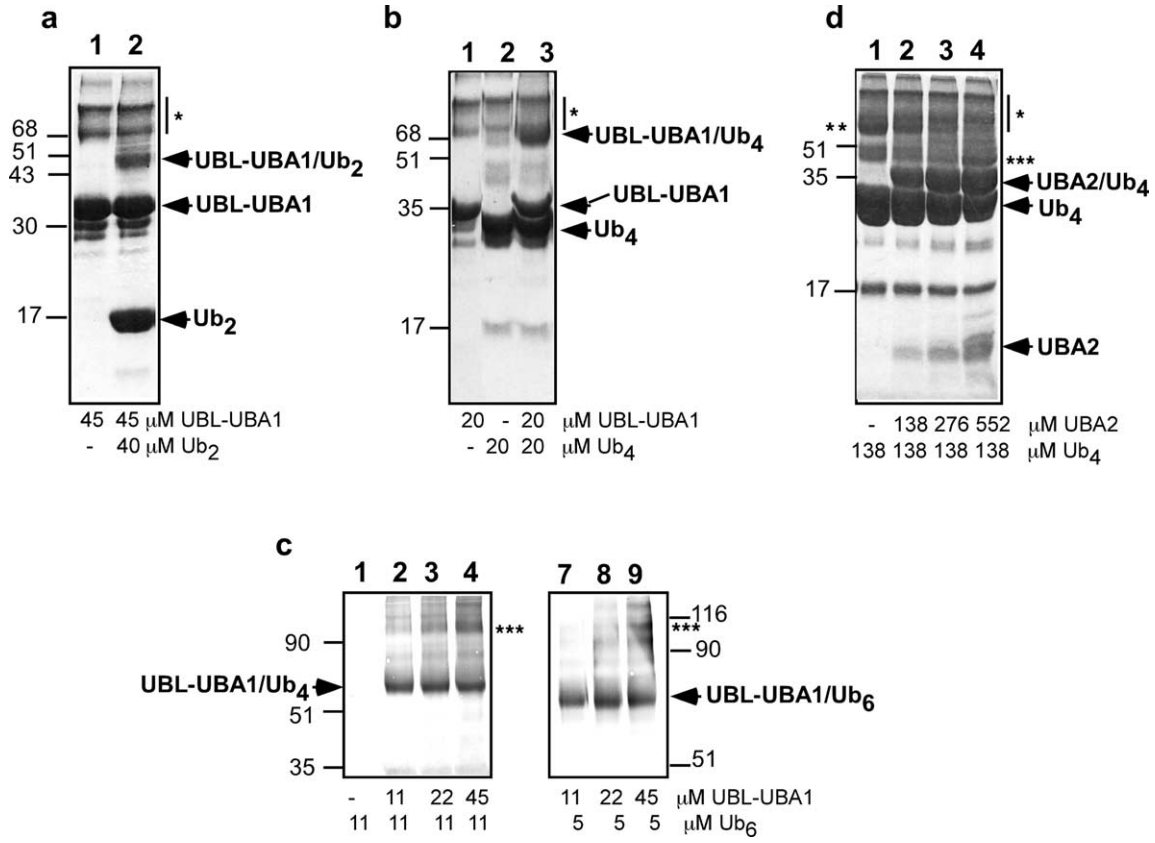

Figure 4. Cross-linking studies (K48-linked chains). Cross-linking reactions were initiated by adding 0.5 mM BS^3 (see Materials and Methods). Compositions of the incubations are given beneath each panel. a, Cross-linking of UBL-UBA1 to Ub_2 (13.5% (w/v) polyacrylamide Coomassie-stained gel). b, Cross-linking of UBL-UBA1 to Ub_4 (12.5% polyacrylamide Coomassie-stained gel). The same result was obtained with 40 μM each UBL-UBA1 and Ub_4 (not shown). c, Cross-linking of UBL-UBA1 to Ub_4 (12.5% gel) and Ub_6 (10% gel; Western blots were developed with anti-HHR23A antibody). Only the region of the blot above non-cross-linked UBL-UBA1 is shown. d, Cross-linking of UBA2 to Ub_4 (13.5% polyacrylamide Coomassie-stained gel). Single asterisks (*) denote products of BSA (carrier) cross-linking. A double asterisk (**) denotes product of weak cross-linking of Ub_4 to itself; this reaction is inhibited at high [UBA2]. Triple asterisks (***) denote possible products of 2 : 1 (UBA/chain) complexes. Numbers to the left or right of the panels are molecular mass markers.

capture on an anti-GST surface (see Materials and Methods). Two such surfaces with different densities displayed highly reproducible binding of Ub_4 (data not shown), yielding $K_d = 1.5$ μM, in good agreement with $K_d = 1.3$ μM obtained with the amine-coupled R23D surface (Figure 5a). However, in comparable studies with Ub_6, the antibody capture surface displayed better reproducibility (results not shown). Therefore, we used the GST-UBA1-2 surface to study the binding of Ub_4, Ub_6 and Ub_8 to a dual-UBA version of HHR23A.

Raw binding data revealed slower association/dissociation kinetics for Ub_6 and Ub_8, compared to Ub_4, on the GST-UBA1-2 surface (Figure 5b, and data not shown). Consistent with this behavior, affinity analysis showed that Ub_6 bound 15-fold more tightly than Ub_4 (Figure 5a, and Table 1). The relatively slow rates of Ub_6 binding and release permitted a kinetic determination of K_d for the GST-UBA1-2/Ub_6 complex. The fits shown in Figure 5b assume values for k_{on} and k_{off} of $2.1 \times 10^6\ M^{-1}s^{-1}$ and $0.1\ s^{-1}$, respectively. The kinetically determined value of K_d (51 nM) is in reasonable agreement with the value (89 nM) determined from the equilibrium analysis. Thus, the binding of UBA1-2 to Ub_6 is 10 to 17-fold tighter than the binding of UBL-UBA1 to the same chain (Table 1), a much larger difference than the approximately twofold tighter binding of short chains to dual *versus* single-UBA proteins (Table 1). We suspect that the stronger relative binding of Ub_6 to the dual-UBA protein reflects the presence of a second binding epitope and the onset of bridging of the two UBA domains at $n = 6$. Further work is needed to prove this model, which could help to explain the higher proteasome inhibition potential of dual-UBA domain versions of HHR23A.[28]

Although data collected with Ub_8 show some deviation from the fit for 1 : 1 binding (Figure 5a), they nonetheless provide an indication that affinity for GST-UBA1-2 approaches a limiting value above $n = 6$. A biphasic dependence of affinity on chain length with single and dual-UBA domain proteins suggests that this feature of the interaction

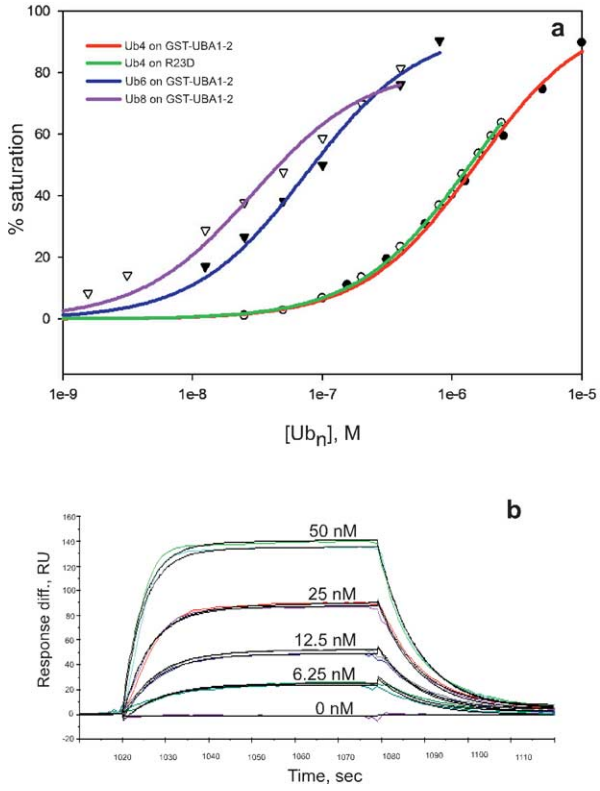

Figure 5. Affinity and kinetic analyses of chain binding to affinity-captured GST-UBA1-2 (SPR). a, K_d determinations for Ub_4, Ub_6, and Ub_8 dissociation from the indicated UBA domain proteins/surfaces (see upper left). See Table 1 for K_d values. b, Global kinetic fit of the Ub_6 interaction with the GST-UBA1-2 surface. The association and dissociation phase data for a subset of Ub_6 concentrations were fit simultaneously using Biacore 3000 BIA-evaluation software (1 : 1, Langmuir model). Black lines represent a fit of the binding data assuming $k_{on}=2.1\times10^6\,M^{-1}\,s^{-1}$, $k_{off}=0.11\,s^{-1}$, and $K_d=51$ nM ($\chi^2=3.46$). Similar values were obtained using the Clamp software (http://www.cores.utah.edu/interaction/clamp.htm).[57]

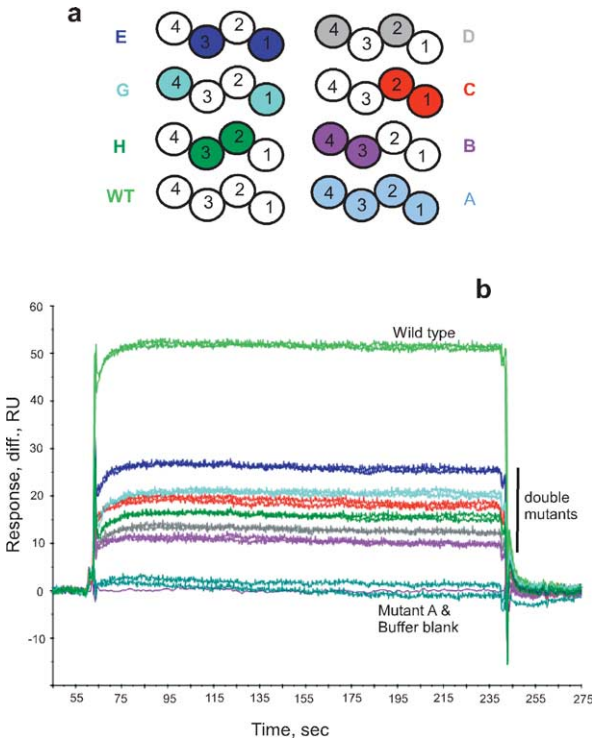

Figure 6. Ub-L8 is important for the interaction of K48-Ub_4 to HHR23A-UBA1 (SPR). a, Schematic representation of Ub_4 molecules used in this experiment. Ub-1 is the proximal moiety (carrying the unconjugated G76), while Ub-4 is the distal moiety (carrying C48). The shaded ubiquitins in each chain carry the L8A mutation, while ubiquitins in white are wild-type. b, Subtracted sensorgrams of interaction of 500 nM solutions of each tetramer (in duplicate) with the UBL-UBA1 surface (surface as in Figure 1). The colors of the different traces correspond to the colors of the letters (and shaded ubiquitins) in a.

reflects a length-dependent property of the chains themselves.

Ubiquitin-L8 is a determinant of K48-Ub_4 binding to UBL-UBA1

Ub-L8 is part of a hydrophobic surface patch that has been implicated in multiple signaling functions of ubiquitin[40,41] and is part of the interface in complexes of monoubiquitin with UBA domains of HHR23A and HHR23B.[32,42] To obtain insight into the role of the ubiquitin patch in polyubiquitin/UBA interactions, we analyzed a series of chimeric K48-Ub_4 molecules, each carrying two Ub-L8A units at different positions (Figure 6a).

A 500 nM solution of each tetramer was used as the analyte in duplicate binding assays on a UBL-UBA1 surface. The all-L8A version of K48-Ub_4 did not interact detectably at this concentration, giving the same response as the injected buffer-blank (Figure 6b, trace A). All of the chimeric tetramers bound detectably to UBL-UBA1, but in all cases they bound more weakly than the wild-type control (Figure 6b). A titration experiment with chimera B confirmed that there was a significant increase in K_d value relative to all-wild-type Ub_4 (about fivefold, data not shown). Because only limited quantities of the chimeras were available, we did not determine K_d values for the other molecules, but each of them is expected to bind as or more tightly than molecule B and more weakly than wild-type Ub_4. In a previous study of the binding of the same chimeric chains to 26 S proteasomes, chimera D and wild-type Ub_4 bound with identical affinities.[48] Thus, the proteasome's polyubiquitin binding site interacts with a subset of the four hydrophobic patches in Ub_4, while all of the L8 side-chains in Ub_4 seem to contribute to the interaction with HHR23A–UBA1 (Figure 6b). In contrast to the marked effects of L8A mutations on the binding of Ub_4 to UBL-UBA1, the affinity of monoubiquitin for HHR23A-UBA1 and UBA2 is unaffected by the L8A mutation.[43]

Competition between polyubiquitin chains and HHR23A-UBL for binding to UBA domains of HHR23A

The UBL domain of intact HHR23A engages in a dynamic intramolecular interaction with both UBA domains.[31] Although bimolecular UBL/UBA interactions are weak ($K_d \sim 2$ mM for the isolated domains of HHR23B[42]), the unimolecular interaction should be much more favorable (Figure 7a). A recent NMR study provided direct evidence that monoubiquitin competes with the UBL domain for access to HHR23A–UBA domains[32] and we previously presented indirect evidence for such competition in the case of polyubiquitin chains.[28] To address the magnitude of the intramolecular UBL/UBA interaction using SPR, we immobilized Ub_6 by amine coupling and compared the binding of HHR23A and R23D, which differ only in the presence or absence of the UBL domain (Figure 1a). R23D bound to the Ub_6 surface with $K_d = 0.15$ μM (Figure 7b). This binding is slightly weaker than $K_d = 0.09$ μM observed for the GST–UBA1-2/Ub_6 complex; the difference may reflect the use of amine-coupled *versus* affinity-captured surfaces (discussed above) or slightly different affinities of R23D *versus* UBA1-2. However, full-length HHR23A bound to the Ub_6 surface significantly more weakly than R23D ($K_d = 0.65$ μM, mean of two determinations; Figure 7b, and data not shown). The fourfold weaker binding of full-length HHR23A is most simply explained by a competitive intramolecular UBL/UBA interaction ($K_x = 4.3$; Figure 7a). If this model is correct, then the necessity to disrupt this interaction will reduce the apparent binding affinity of polyubiquitin chains by ~4-fold (Figure 7a).

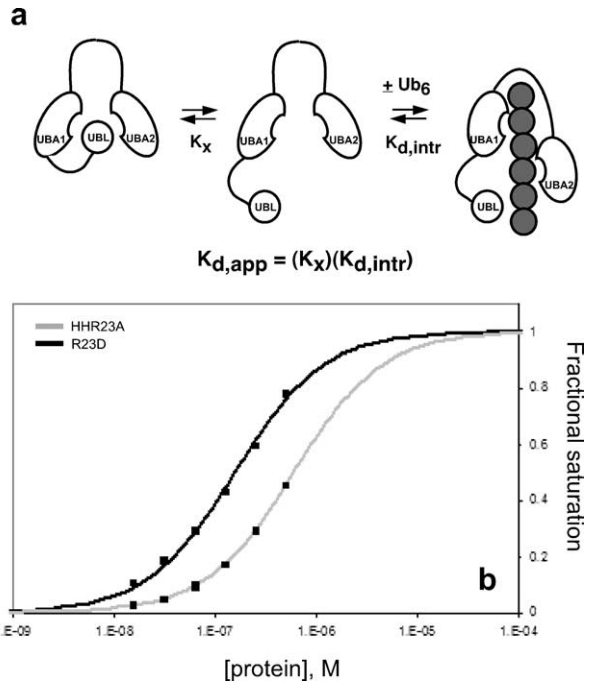

Figure 7. UBL domain of HHR23A interferes with the UBA/Ub_6 interaction (SPR). a, Model for intramolecular UBL/UBA interactions (left) and intermolecular binding of Ub_6 (right), assuming that the UBL domain dissociates (center) before Ub_6 binds. The $K_{d,intr}$ value is assumed to be equal to the K_d value of the R23D/Ub_6 complex (0.15 μM; b) allowing K_x to be calculated based on $K_{d,app}$ for the HHR23A/Ub_6 complex (0.65 μM; b). The UBA domains in the right-most complex could interact with any ubiquitin in the chain. b Full-length HHR23A (gray line) or its UBL-deleted mutant R23D (black line) were used as analyte on an amine-coupled Ub_6 surface. Data were analyzed as for Figure 1c. The lines were calculated assuming $K_d = 0.15$ μM (black line) or 0.65 μM (gray line).

At present we do not know if there is an interaction between the UBL and UBA domains of UBL-UBA1. We were unable to address this question due to unexpected properties of the isolated UBA1 domain (discussed above). The value of K_x (dissociation constant of the intramolecular interaction) determined in Figure 7 represents an upper limit on the affinity of any intramolecular UBL/UBA interaction in UBL-UBA1 (in fact a value of $K_x/2$ is expected because there is only one UBA domain). There is no reason to suspect that such an effect would alter the length dependence or stoichiometry of chain binding to UBL-UBA1.

The proteasome-inhibitory activity of native full-length HHR23A is significantly less than that of native R23D, but the activities of the two proteins are equalized by heat treatment through a specific increase in inhibition by full-length HHR23A.[28] We speculated that heating disrupted the UBL/UBA interaction, freeing the UBA domain(s) to bind substrate-linked polyubiquitin chains and interfere with targeting to proteasomes. The current results (Figure 7b) provide further experimental support for this proposal, but pull-down assays comparing GST-HHR23A to GST-R23D did not reveal a strong difference in chain binding.[28] The discrepancy can be explained by disruption of the intramolecular UBL/UBA interaction upon fusion of the UBL to GST. In this case, GST-HHR23A will display its full chain-binding potential, as observed in our previous work.

Discussion

Our data reveal several distinctive properties of HHR23A-UBA/polyubiquitin complexes. First, we confirm that the strength of the interaction depends on the chemical structure of the chain. Here, we used UBL-UBA1/Ub_4 complexes to show that the linkage specificity of this truncated protein reflects a five- to tenfold difference in the K_d values of the two chains (Figure 1). This linkage preference is retained when both UBA domains are present.[28] A preference for the K48 linkage also applies in the binding of Ub_2 to GST-UBA2,[49] indicating that this property is qualitatively independent of chain length.

In contrast, and as shown here for the first time, affinity depends strongly on chain length. The equilibrium dissociation constants for UBL-UBA1/Ub_n

complexes decrease approximately exponentially between $n=1$ and $n=4$, but there is little further change above $n=6$ (Figure 2c). The K_d values for UBA1-2/Ub_n complexes also appear to approach a limit as the chain gets longer (Table 1), although these data are less extensive and interactions with long chains exhibit some qualitative differences in behavior (discussed above). Cross-linking and sedimentation equilibrium analyses revealed that a 1 : 1 (mol/mol) stoichiometry predominates in the binding of UBL-UBA1 to chains of $n=2$–6 (Figures 3 and 4). Finally, our results suggest that each L8 residue in K48-Ub_4 contributes to binding (Figure 6). These properties of UBA/Ub_ncomplexes place significant constraints on the mode of interaction, as discussed below.

SPR proved to be an important tool in this work. The high sensitivity and reproducibility of this technique counteracts the limitations introduced by the difficulties of chain synthesis, especially above $n=4$. Ubiquitin, polyubiquitin chains, and UBA domains are generally easy to refold, allowing amine-coupled surfaces to be re-used many times without significant loss of signal. SPR should provide a convenient and sensitive method to monitor polyubiquitin interactions with more complex ligands in future studies.

To date, structural studies have been limited to complexes of UBA domains with monoubiquitin. In the three published examples, a surface hydrophobic patch of the UBA domain contacts a surface epitope of ubiquitin that includes the L8 and I44 side-chains.[31,42,43] Although it is attractive to postulate that such an interaction could be replicated along the length of the chain, several observations preclude this "one-UBA-per-ubiquitin" model for polyubiquitin chain binding by the model UBA domain proteins studied here. First, the side-chain of K48 is occluded by the bound UBA domain in the monoubiquitin/UBA complexes, arguing that this mode of interaction is unlikely to apply to K48-linked chains.[32,42,43] Conversely, in the predominant conformation of K48-Ub_2 seen in solution at neutral pH, there is mutual occlusion of the two L8 and I44 side-chains.[51] This interface is also seen in Ub_4, although the detailed solution conformation of K48-Ub_4 remains to be determined.[51] Even though this interface is dynamic[51] and cannot be uniformly repeated in Ub_4 and longer chains, it is still the case that any use of ubiquitin's hydrophobic patch for ubiquitin/ubiquitin contacts will impede a simple one-UBA-per-ubiquitin mode of interaction. This simple model also fails to predict the initial exponential increase in affinity with increasing chain length (Figure 3c). The different effects of the Ub-L8A mutation on the UBL-UBA1/Ub_4 interaction (Figure 6, inhibitory) and the UBA1/mono-ubiquitin interaction (benign[43]) further contradict this model. Finally, HHR23A-UBL-UBA1 and UBA2 bind to Ub_4 with a 1 : 1 (mol/mol) stoichiometry (Figures 3 and 4). In contrast, the one-UBA-per-ubiquitin model predicts a 4 : 1 stoichiometry for these complexes. Our results provide a hint that chains that are more than six ubiquitin molecules in length may be able to bind both UBA domains of HHR23A. Structural studies, in progress, will aid greatly in determining the merit of this model.

Although further work is needed to determine exactly how K48-linked chains bind to HHR23A-UBA domains, the present data show that HHR23A-UBL-UBA1 binds nearly optimally to Ub_4 or Ub_6. More limited data obtained with UBA1-2 suggest that this is also true when two UBA domains are present. We propose that a K48-linked chain of this length presents one or more interaction surfaces that are incomplete or absent in shorter chains, presumably due to unique conformational features of K48-linked chains. Indeed, NMR studies have shown that the solution conformations of K48- and K63-Ub_2 are distinct, the K48-linked dimer adopts the closed conformation discussed above, whereas the K63-linked dimer adopts an open, extended conformation in which both patches are solvent-exposed.[49,51] To explain why all of the L8 residues in Ub_4 contribute to UBA binding (Figure 6), we propose that certain L8 side-chains directly contact the UBA domain, while others play an indirect role by stabilizing the conformation of the chain. Structural studies are needed to address this model rigorously.

The pronounced dependence of affinity on chain length helps to explain why UBA domain proteins associate predominantly with very high molecular mass conjugates *in vivo*.[20,26,44,52] Interestingly, the length dependence of K48 chain binding to 26 S proteasomes is also biphasic with a breakpoint near $n=4$, a result that can also be explained by the model discussed above.[48] Ub-L8 is important for the binding of K48-linked chains to the proteasome's 19 S complex,[40] but in contrast to the UBL-UBA1/Ub_4 interaction, only a subset of the L8 residues in Ub_4 are important for proteasome binding.[48] It remains to be determined if this difference reflects the interaction of UBA domains and proteasomes with different surfaces of a similarly folded chain or if the conformations of the bound chain differs between the two complexes.

Although the one-UBA-per-ubiquitin model cannot explain the interactions studied here, it may hold for other chains and/or other UBA domains. A recent docking study suggested how the minimal UBA domains of HHR23A could bind in several different orientations to monoubiquitin; even more versatility might be expected when comparing UBA domains from different proteins.[43] For example, the Vps9-CUE domain binds monoubiquitin as a dimer and this mode of interaction suggests how multiple UBA domains could bind to a single chain.[38] (However, the isolated UBA domains of HHR23A and B are monomeric,[32,35,42] as confirmed by our cross-linking and ultracentrifugation data.) Also, our studies of the binding of K63-Ub_2 to HHR23A-UBA2 domain revealed that two UBA domains can bind weakly to one molecule of K63-Ub_2, in each case through a hydrophobic

interface.[49] This mode of interaction is likely to be determined by the simple, extended conformation of the K63-linked chain, which contrasts with the more complex conformation(s) adopted by K48-linked chains.[49,51] Our studies of UBA/polyubiquitin interactions suggest that the conformation of the chain is a major determinant of the mode of interaction.

The modular structure of HHR23A[31] suggests that UBA/polyubiquitin interactions should be qualitatively similar in truncated and full-length HHR23A and B, except that intramolecular UBL/UBA interactions will hinder bimolecular interactions of the UBL and UBA domains in the full-length proteins. Our data indicate that the favorable intramolecular interaction will reduce the apparent affinity of polyubiquitin chains by about fourfold. The binding of mono- or polyubiquitin to the UBA domains will promote the binding of the UBL domain to ligands such as the proteasome subunits S2 and S5a/Rpn10, while the latter interaction will promote the binding of (poly)ubiquitin, or other ligands such as HIV-Vpr protein, to the UBA domains.[28,31–33] Whether the UBA or UBL domain is engaged "first" will depend on the K_d value of each bimolecular interaction relative to the concentration of the relevant ligand. Thus, intramolecular UBL/UBA interactions will further modulate intracellular signaling mediated by bimolecular (poly)-ubiquitin/UBA interactions.

Materials and Methods

Recombinant proteins

Wild-type and mutant ubiquitins were expressed in bacteria and purified as described.[53] K48-linked chains of $n=2$–12 were synthesized stepwise starting from Ub-K48C and Ub-D77 and purified by FPLC to near-homogeneity.[48] In the experiment shown in Figure 1 (see Results), the C48 residue of the distal ubiquitin in K48-Ub_4 was alkylated with iodoacetamide. In other experiments, the C48 residue was unmodified. (The distal ubiquitin is the one that ordinarily would carry the unconjugated lysine residue.) K63-Ub_4 was synthesized as described in our previous work and carried R63 in the distal ubiquitin.[54] Chain concentrations were determined from UV absorbance.[53] The chimeric tetramers used in Figure 6 (see Results) are the same molecules used in a previous study.[48] Western blots were developed with rabbit anti-HHR23A antiserum (1 : 1000) (a gift from P. Howley) and immune complexes were visualized using alkaline phosphatase-conjugated secondary antibody (BioRad).

The versions of HHR23A used here (Figure 1a) were called HHR23A (full-length protein), R23D (residues 77–363), UBA1-2 (residues 158–363), UBL-UBA1 (residues 2–211, plus ten C-terminal residues introduced during cloning (LGRLERPHRD)), UBA1 (residues 159–211, plus the same extra residues present in UBL-UBA1), and UBA2 (residues 315–363). R23D, UBA1-2, UBL-UBA1, and UBA1 also have two extra N-terminal residues (GS), which are a residue of the thrombin site. In UBA2, three alanine residues follow the GS dyad. All versions of HHR23A were expressed as GST-fusion proteins, cleaved with thrombin, and FPLC-purified as described,[28] except that the small (~50 residues) UBA1 and UBA2 domains were purified by gel-filtration on a Superose 12 FPLC column (Amersham-Pharmacia Biotech). In some SPR experiments, GST-UBA1-2 was used as an intact fusion protein. UBA protein purity was determined by SDS-PAGE to be >90%. Proteins were diluted or dialyzed in HBS buffer (pH 7.5), when necessary, to minimize differences in bulk refractive index in SPR studies.

SPR measurements

SPR studies were performed on a Biacore 3000 instrument. Sensor chips CM5, NHS/EDC coupling reagents, ethanolamine, anti-GST monoclonal antibody, and HBS-EP buffer (see below) were from Biacore AB (Uppsala, Sweden). Most binding assays were performed by amine-coupling UBL-UBA1 or R23D in acetate buffer (pH 4.5–5.0) to sensor chip CM5 at a moderately low density (R_L=200–300 RU), with polyubiquitin chains used as analyte in the mobile phase. A mock-immobilized surface was used as a control in each individual affinity analysis and non-specific binding was found to be minimal. The expected value of R_{max} in these studies ranged from ~250 to 800 RU, depending on the mass of the analyte, and observed values were in good agreement with expectation. For studies of chain binding to UBA1 and UBA2, we amine-coupled Ub_6 (acetate buffer, pH 5.5) on a CM5 chip to R_L~3000 RU and used the UBA domains as analytes. For experiments addressing the effect of the UBL on chain binding, we amine-coupled Ub_6 to R_L~6000 RU and used either HHR23A or R23D as analyte. Generally we used 10 mM glycine (pH 2.2) as the regeneration buffer with amine-coupled surfaces. The properties of UBA domain and chain surfaces remained constant through multiple rounds of regeneration as determined by a reproducible response in a control binding assay conducted after each round of regeneration. For studies involving affinity capture of the ligand we amine-coupled the anti-GST antibody to RU~5000. GST-UBA1-2 was then captured at ~200 or ~700 RU on this surface.

Binding experiments were performed in HBS-EP buffer (10 mM Hepes (pH 7.5), 150 mM NaCl, 3 mM EDTA, 0.005% (v/v) Surfactant P20 (pH 7.4)) at 25 °C. Equilibrium analyses utilized a flow rate of 30 μl/minute, with analyte concentrations ranging from low-nanomolar to high-micromolar (see the Figure legends). A mock-immobilized surface in the reference flow cell enabled us to subtract changes in bulk refractive index during binding; we routinely monitored the interaction at each analyte concentration at least in duplicate. For K_d determinations, analyte solutions were generally injected for two minutes. Equilibrium binding levels were determined by averaging the responses between 20 seconds and 40 seconds before the injection was stopped. Experimental equilibrium responses and R_{max} values were used to calculate fractional saturation values, which were plotted against analyte concentration and fit by non-linear least-squares analysis to a non-cooperative 1 : 1 ligand binding model with Sigmaplot 8.0 software. Similar values of K_d were obtained using Global Analysis of a steady-state affinity model (BIAevaluation software). In most cases, data and theoretical fits were plotted using Microsoft Excel.

Cross-linking

The homo-bifunctional amine-reactive cross-linker BS^3 was purchased from Pierce. Cross-linking incubations

contained Hepes-buffered saline (HBS) (pH 7.5), bovine serum albumin (BSA) as a carrier (200 μg/ml), and UBA domain protein and polyubiquitin chains as indicated in the legend to Figure 4. Reactions were initiated by adding 0.5 mM BS^3 (freshly prepared) and terminated after 15 minutes (room temperature) with SDS-PAGE sample buffer (shown in controls to be equivalent to quenching with 50 mM Tris base). To avoid non-specific aggregation of polyubiquitin chains, samples were boiled for just five seconds prior to loading.

Analytical unltracentrifugation

Sedimentation equilibrium analytical ultracentrifugation experiments were performed using a Beckman XL-A analytical ultracentrifuge equipped with absorbance optics. Sedimentation equilibrium data for Ub_4 and UBL-UBA1 were collected at three protein concentrations in six-sector cells at 24,500, 30,000 and 37,000 rpm for lengths of time sufficient to reach equilibrium. Nine equilibrium data sets for each protein were globally fit using the WinNonlin algorithm.[55] To determine the stoichiometry and equilibrium constant for the UBL-UBA1/Ub_4 interaction, sedimentation equilibrium experiments were carried out on a 1 : 2 (UBL-UBA1/Ub_4) molar ratio mixture of the two proteins. Equilibrium data at 20,000, 24,500 and 30,000 rpm for three total protein concentrations were collected. These nine data sets were globally fit using Igor Pro software with user-programmed sedimentation equilibrium equations describing a 1 : 1 or 2 : 1 or 4 : 1 (UBA-UBL1/Ub_4) binding complex between the molecules assuming additivity for the partial specific volumes and molar extinction coefficients of the complexes. For all experiments, the values of the partial specific volume, solvent density and molecular mass were calculated from the amino acid compositions using the Sednterp algorithm.[56]

Acknowledgements

This work was supported by grants to C.M.P. from the NIH (DK46984) and to K.G.F. from a Department of Defence Career Development Award (DAMD 17-02-1-0427) and the NIH (GM57534). We thank R. Cohen, D. Fushman, and M. Eddins for comments on the manuscript, and JoAnne Bruno for helpful discussions. We are grateful to P. Howley for a generous gift of anti-HHR23A antiserum.

Supplementary data

Supplementary data associated with this article can be found, in the online version, at doi:10.1016/j.jmb.2004.06.057

References

1. Hershko, A. & Ciechanover, A. (1998). The ubiquitin system. *Annu. Rev. Biochem.* **67**, 425–479.
2. Pickart, C. M. (2001). Mechanisms underlying ubiquitination. *Annu. Rev. Biochem.* **70**, 503–533.
3. Peng, J., Schwartz, D., Elias, J. E., Thoreen, C. C., Cheng, D., Marsischky, G. *et al*. (2003). A proteomics approach to understanding protein ubiquitination. *Nature Biotechnol.* **21**, 921–926.
4. Baumeister, W., Walz, J., Zuhl, F. & Seemuller, E. (1998). The proteasome: paradigm of a self-compartmentalizing protease. *Cell*, **92**, 367–380.
5. Chau, V., Tobias, J. W., Bachmair, A., Marriott, D., Ecker, D. J., Gonda, D. K. & Varshavsky, A. (1989). A multiubiquitin chain is confined to specific lysine in a targeted short-lived protein. *Science*, **243**, 1576–1583.
6. Finley, D., Sadis, S., Monia, B. P., Boucher, P., Ecker, D. J., Crooke, S. T. & Chau, V. (1994). Inhibition of proteolysis and cell cycle progression in a multiubiquitination-deficient yeast mutant. *Mol. Cell. Biol.* **14**, 5501–5509.
7. Johnson, E. S., Ma, P. C., Ota, I. M. & Varshavsky, A. (1995). A proteolytic pathway that recognizes ubiquitin as a degradation signal. *J. Biol. Chem.* **270**, 17442–17456.
8. Spence, J., Sadis, S., Haas, A. L. & Finley, D. (1995). A ubiquitin mutant with specific defects in DNA repair and multiubiquitination. *Mol. Cell. Biol.* **15**, 1265–1273.
9. Hofmann, R. M. & Pickart, C. M. (1999). Noncanonical MMS2-encoded ubiquitin-conjugating enzyme functions in assembly of novel polyubiquitin chains for DNA repair. *Cell*, **96**, 645–653.
10. Hoege, C., Pfander, B., Moldovan, G.-L., Pyrowolakis, G. & Jentsch, S. (2002). *RAD6*-dependent DNA repair is linked to modification of PCNA by ubiquitin and SUMO. *Nature*, **419**, 135–141.
11. Deng, L., Wang, C., Spencer, E., Yang, L., Braun, A. You, J. *et al*. (2000). Activation of the IκB kinase complex by TRAF6 requires a dimeric ubiquitin-conjugating enzyme complex and a unique polyubiquitin chain. *Cell*, **103**, 351–361.
12. Spence, J., Gali, R. R., Dittmar, G., Sherman, F., Karin, M. & Finley, D. (2000). Cell cycle-regulated modification of the ribosome by a variant multiubiquitin chain. *Cell*, **102**, 67–76.
13. You, J. & Pickart, C. M. (2001). A Hect domain E3 enzyme assembles novel poly-ubiquitin chains. *J. Biol. Chem.* **276**, 19871–19878.
14. Hofmann, K. & Bucher, P. (1996). The UBA domain: a sequence motif present in multiple enzyme classes of the ubiquitination pathway. *Trends Biochem. Sci.* **21**, 172–173.
15. Hofmann, K. & Falquet, L. (2001). A ubiquitin-interacting motif conserved in components of the proteasomal and lysosomal protein degradation systems. *Trends Biochem. Sci.* **26**, 347–350.
16. Ponting, C. P. (2000). Proteins of the endoplasmic-rticulum-associated degradation pathway: domain detection and function prediction. *Biochem. J.* **351**, 527–535.
17. Vadlamudi, R. K., Joung, I., Strominger, J. L. & Shin, J. (1996). p62, a phopshotyrosine-independent ligand of the SH2 domain of $p56^{lck}$, belongs to a new class of ubiquitin-binding proteins. *J. Biol. Chem.* **271**, 20235–20237.
18. Bertolaet, B. L., Clarke, D. J., Wolff, M., Watson, M. H., Henze, M., Divita, G. & Reed, S. I. (2001). UBA domains of DNA damage-inducible proteins interact with ubiquitin. *Nature Struct. Biol.* **8**, 417–422.
19. Chen, L., Shinde, U., Ortolan, T. G. & Madura, K. (2001). Ubiquitin-associated (UBA) domains in

Rad23 bind ubiquitin and promote inhibition of multi-ubiquitin chain assembly. *EMBO Rep.* **2**, 933–938.
20. Wilkinson, C. R. M., Seeger, M., Hartmann-Petersen, R., Stone, M., Wallace, M., Semple, C. & Gordon, C. (2001). Proteins containing the UBA domain are able to bind multi-ubiquitin chains. *Nature Cell Biol.* **3**, 939–943.
21. Walters, K. J., Kleijnen, M. F., Goh, A. M., Wagner, G. & Howley, P. M. (2002). Structural studies of the interaction between ubiquitin family proteins and proteasome subunit S5a. *Biochemistry,* **41**, 1767–1777.
22. Schauber, C., Chen, L., Tongaonkar, P., Vega, I., Lambertson, D., Potts, W. & Madura, K. (1997). Rad23 links DNA repair to the ubiquitin/proteasome pathway. *Nature*, **391**, 715–718.
23. Elsasser, S., Gali, R. R., Schwickart, M., Larsen, C. N., Leggett, D. S. Muller, B. *et al*. (2002). Proteasome subunit Rpn1 binds ubiquitin-like protein domains. *Nature Cell Biol.* **4**, 725–730.
24. Hartmann-Petersen, R., Seeger, M. & Gordon, C. (2003). Transferring substrates to the 26S proteasome. *Trends Biochem. Sci.* **28**, 26–31.
25. Lambertson, D., Chen, L. & Madura, K. (1999). Pleiotropic defects caused by loss of the proteasome-interacting factors Rad23 and Rpn10 of *Saccharomyces cerevisiae*. *Genetics*, **153**, 69–79.
26. Funakoshi, M., Sasaki, T., Nishimoto, T. & Kobayashi, H. (2002). Budding yeast Dsk2p is a polyubiquitin-binding protein that can interact with the proteasome. *Proc. Natl Acad. Sci. USA*, **99**, 745–750.
27. Rao, H. & Sastry, A. (2002). Recognition of specific ubiquitin conjugates is important for the proteolytic functions of the UBA domain proteins Dsk2 and Rad23. *J. Biol. Chem.* **277**, 11691–11695.
28. Raasi, S. & Pickart, C. M. (2003). Rad23 ubiquitin-associated domains (UBA) inhibit 26S proteasome-catalyzed proteolysis by sequestering lysine 48-linked polyubiquitin chains. *J. Biol. Chem.* **278**, 8951–8959.
29. Lommel, L., Ortolan, T., Chen, L., Madura, K. & Sweder, K. S. (2002). Proteolysis of a nucleotide excision repair protein by the 26S proteasome. *Curr. Genet.* **42**, 9–20.
30. Ng, J. M. Y., Vermeulen, W., van der Horst, G. T. J., Bergink, S., Sugasawa, K., Vrieling, H. & Hoeijmakers, J. H. J. (2003). A novel mechanism of DNA reapir by damage-induced and RAD23-dependent stabilization of xeroderma pigmentosum group C protein. *Genes Dev.* **17**, 1630–1645.
31. Walters, K. J., Lech, P. J., Goh, A. M., Wang, Q. & Howley, P. M. (2003). DNA-repair protein hHR23a alters its protein structure upon binding proteasomal subunit S5a. *Proc. Natl Acad. Sci. USA*, **100**, 12694–12699.
32. Wang, Q., Goh, A. M., Howley, P. M. & Walters, K. J. (2003). Ubiquitin recognition by the DNA repair protein hHR23A. *Biochemistry*, **42**, 13529–13535.
33. Dieckmann, T., Withers-Ward, E. S., Jarosinski, M. A., Liu, C.-F., Chen, I. S. Y. & Feigon, J. (1998). Structure of a human DNA repair protein UBA domain that interacts with HIV-1 Vpr. *Nature Struct. Biol.* **5**, 1042–1047.
34. Withers-Ward, E. S., Mueller, T. D., Chen, I. S. Y. & Feigon, J. (2000). Biochemical and structural analysis of the interaction between the UBA(2) domain of the DNA repair protein HHR23A and Vpr. *Biochemistry,* **39**, 14103–14112.
35. Mueller, T. D. & Feigon, J. (2002). Solution structures of UBA domains reveal a conserved hydrophobic surface for protein–protein interactions. *J. Mol. Biol.* **319**, 1243–1255.
36. Ciani, B., Layfield, R., Cavey, J. R., Sheppard, P. W. & Searle, M. S. (2003). Structure of the UBA domain of p62 (SQSTM1) and implications for mutations which cause Paget's disease of bone. *J. Biol. Chem.* **278**, 37409–37412.
37. Kang, R. S., Daniels, C. M., Francis, S. A., Shih, S. C., Salerno, W. J., Hicke, L. & Radhakrishnan, I. (2003). Solution structure of a CUE-mono-ubiquitin complex reveals a conserved mode of ubiquitin binding. *Cell*, **113**, 621–630.
38. Prag, G., Misra, S., Jones, E. A., Ghirlando, R., Davies, B. A., Horazdovsky, B. F. & Hurley, J. H. (2003). Mechanism of ubiquitin recognition by the CUE domain of Vps9p. *Cell*, **113**, 609–620.
39. Vijay-Kumar, S., Bugg, C. E. & Cook, W. J. (1987). Structure of ubiquitin refined at 1.8 Å resolution. *J. Mol. Biol.* **194**, 531–544.
40. Beal, R. E., Toscano-Cantaffa, D., Young, P., Rechsteiner, M. & Pickart, C. M. (1998). The hydrophobic effect contributes to polyubiquitin chain recognition. *Biochemistry*, **37**, 2925–2934.
41. Sloper-Mould, K. E., Jemc, J., Pickart, C. M. & Hicke, L. (2001). Distinct functional surface regions on ubiquitin. *J. Biol. Chem.* **276**, 30483–30489.
42. Ryu, K.-S., Lee, K.-J., Bae, S.-H., Kim, B.-K., Kim, K.-A. & Choi, B.-S. (2003). Binding surface mapping of intra and inter domain interactions among HHR23B, ubiquitin, and polyubiquitin binding site 2 of S5a. *J. Biol. Chem.* **278**, 36621–36627.
43. Mueller, T. D., Kamionka, M. & Feigon, J. (2004). Specificity of the interaction between ubiquitin-associated domains and ubiqtuitin. *J. Biol. Chem.* **279**, 11926–11936.
44. Saeki, Y., Saitoh, A., Toh-e, A. & Yokosawa, H. (2002). Ubiquitin-like proteins and Rpn10 play cooperative roles in ubiquitin-dependent proteolysis. *Biochem. Biophys. Res. Commun.* **293**, 986–992.
45. Van Regenmortel, M. H. (2003). Improving the quality of BIACORE-based affinity measurements. *Dev. Biol.* **112**, 141–151.
46. Myszka, D. G. (1999). Improving biosensor analysis. *J. Mol. Recogn.* **12**, 279–284.
47. Morton, T. A. & Myszka, D. G. (1998). Kinetic analysis of macromolecular interactions using surface plasmon resonance biosensors. *Methods Enzymol.* **295**, 268–294.
48. Thrower, J. S., Hoffman, L., Rechsteiner, M. & Pickart, C. M. (2000). Recognition of the polyubiquitin proteolytic signal. *EMBO J.* **19**, 94–102.
49. Varadan, R., Assfalg, M., Haririnia, A., Raasi, S., Pickart, C. M. & Fushman, D. (2004). Solution conformation of Lys^{63}-linked di-ubiquitin chain provides clues to functional diversity of polyubiquitin signaling. *J. Biol. Chem.* **279**, 7055–7063.
50. Chen, L. & Madura, K. (2002). Rad23 promotes the targeting of proteolytic substrates to the proteasome. *Mol. Cell. Biol.* **22**, 4902–4913.
51. Varadan, R., Walker, O., Pickart, C. M. & Fushman, D. (2002). Structural properties of polyubiquitin chains in solution. *J. Mol. Biol.* **324**, 637–647.
52. Lambertson, D., Chen, L. & Madura, K. (2003). Investigating the importance of proteasome-interaction for Rad23 function. *Curr. Genet.* **42**, 199–208.
53. Piotrowski, J., Beal, R., Hoffman, L., Wilkinson, K. D., Cohen, R. E. & Pickart, C. M. (1997). Inhibition

of the 26 S proteasome by polyubiquitin chains synthesized to have defined lengths. *J. Biol. Chem.* **272**, 23712–23721.
54. Hofmann, R. M. & Pickart, C. M. (2001). *In vitro* assembly and recognition of K63 poly-ubiquitin chains. *J. Biol. Chem.* **276**, 27936–27943.
55. Johnson, M. L., Correia, J. J., Yphantisl, D. A. & Halvorson, H. R. (1981). Analysis of data from the analytical ultracentrifuge by non-linear least-squares techniques. *Biophys. J.* **36**, 575–588.
56. Laue, T. M., Shah, X., Ridgeway, T. M., Pelletier, S. L. (1992). Computer-aided interpretation of analytical sedimentation data for proteins. In *Analytical Ultracentrifugation in Biochemistry and Polymer Science*, pp. 90–125, Royal Society of Chemistry, Cambridge, UK.
57. Myszka, D. G. (1998). CLAMP: a biosensor kinetic data analysis program. *Trends Biochem. Sci.* **23**, 149–150.

Edited by S. Reed

(Received 22 December 2003; received in revised form 13 April 2004; accepted 7 June 2004)